Korean J. Chem. Eng., 34(2), 574-579 (2017)
DOI: 10.1007/s11814-016-0338-5

pISSN: 0256-1115
eISSN: 1975-7220

Comparative experimental study of ethanol-air premixed laminar combustion characteristics by laser induced spark and electric spark ignition

Cangsu Xu*,†, Yangyang Hu*, Xiaolu Li, Xuan Zhou*, and Anhao Zhong***

*College of Energy Engineering, Zhejiang University, Hangzhou 310027, China
**College of Mechanical and Electrical Engineering, China Jiliang University, Hangzhou 310018, China
(*Received 1 July 2016 • accepted 29 November 2016*)

Abstract−An experimental study of laminar combustion characteristics of ethanol-air premixed mixtures was conducted with different ignition methods, including laser induced spark ignition (LISI) and electric spark ignition (SI) at an initial condition of 358 K temperature and 0.1 MPa pressure. Flame propagation with the two different ignition methods was analyzed and discussed. The laminar flame speed was extrapolated with a nonlinear extrapolation method. Results indicate that the laminar speed of ethanol-air mixtures with LISI is faster than that with SI at lean mixtures, but slower at stoichiometric and rich mixtures. The peak values of the laminar burning velocity for SI and LISI with nonlinear extrapolation are 50.1 cm/s and 47.6 cm/s at the equivalence ratio of 1.1, respectively. Laser-induced spark ignition is able to ignite leaner ethanol-air mixtures.

Keywords: Laser Induced Spark Ignition (LISI), Electric Spark Ignition (SI), Laminar Flame Speed, Propagating Spherical Flame, Ethanol

INTRODUCTION

Due to increased environmental awareness, more rigorous emission regulations, and challenges of sustainable energy supply, the development of internal combustion engines with high efficiencies and low emissions has become the focus of engine researchers. To reduce greenhouse gases emission from transportation sectors, promising alternative fuels such as methanol [1,2] and ethanol [3,4] have been investigated. Ethanol, which is used as an octane booster for gasoline [5], is known to have a higher flame propagation velocity than that of gasoline [6]. It has a lower combustion temperature, which reduces the heat loss to the combustion chamber. Therefore, ethanol potentially leads to high engine thermal efficiencies [7]. Lean combustion in internal combustion engines has the potential to improve fuel economy and reduce emissions. However, there are many challenges in applying lean combustion strategy into practice. Ignition-related problems, such as the sluggish flame initiation and propagation, can lead to unstable combustion, and to some extent, even engine misfire [8]. Thus, a new ignition technology is vital to the successful implementation of the lean combustion technology.

Laser ignition [8-12] has become a hot research topic because of its advantages over conventional electric spark ignition (SI), including better controls over the timing and locations of ignition. Laser-induced spark ignition systems have no electrodes, which potentially leads to a longer lifetime. What's more, laser-induced spark ignition (LISI) can achieve multi-point ignition, accelerating the combustion of lean mixtures. Dietmar Boker and Dieter Bruggemann [12] showed that it was possible to localize the laser ignition adaptively to get optimum ignition conditions in an inhomogeneous mixture, which means that LISI allows for an adaptive control of combustion for lower emissions and higher efficiency in various engine operating conditions. However, one of the main disadvantages of LISI is that energy conversion efficiency of a laser system is still not high enough and only a part of the laser energy is absorbed by the gaseous medium in the vicinity of the ignition location [8].

To compare LISI and SI under laboratory conditions, Srivastava et al. [10] conducted an experiment at an initial pressure of 3 MPa and an initial temperature of 323 K in a constant volume combustion chamber; the results showed that LISI led to a higher pressure rise rate inside the combustion chamber, due to the absence of a plasma quenching effect with laser ignition. Other researchers also found that laser ignition led to shorter ignition delay and shorter combustion duration compared with SI [13,14]. Rahman et al. [15] studied combustion characteristics of wet ethanol ignited using a focused Q-switched Nd:YAG nanosecond laser. They concluded that the flame luminosity, flame growth rate, and flame propagation speed increased by the addition of 10 vol% and 20 vol% water, indicating a potential positive effect of water addition. Ambrós et al. [3] did experimental analysis and modeling of an internal combustion engine operating with wet ethanol, proving that the engine was capable of operating with mixtures of wet ethanol up to 40 vol% water.

However, there are limited data or publications available for comparing the combustion characteristics of ethanol with LISI and SI. Thus, our research objective was to investigate the combustion process and laminar burning speeds of ethanol-air mixtures with LISI

†To whom correspondence should be addressed.
E-mail: xucangsu@zju.edu.cn
‡This paper is reported in the 11th China-Korea Clean Energy Workshop.

and SI. The results of flame propagation progress, laminar flame speed and the radiation effect on the flame propagation are discussed, and an assumption is given to explain the different ethanol-air premixed laminar flame speeds by LISI and SI.

EXPERIMENTAL SETUP AND PROCEDURES

1. Experimental Setup

Fig. 1 and Fig. 2 show schematics of the experimental apparatuses for SI and LISI, respectively. The temperature of constant volume combustion chamber is controlled by six resistance heaters in each walls and a proportional-integral-derivative (PID) controller. The volumes of the constant volume combustion bomb with SI and LISI are 1.94 L and 2.14 L, respectively. For the purpose of optical access, three pairs of orthogonal windows with diameters of 105 mm are available at six sides of the chamber. Two opposing electrodes (platinum wires with a diameter of 0.4 mm) are used as a spark plug along with an ignition coil and a control module. The laser beam is focused in the chamber by a spherically corrected convex lens with a focal length of 500 mm, and the absorbed energy deposited in the plasma is calculated based on the measurements of laser energy sensors. More details about the parameters of the focused laser and formula of laser ignition energy can be found in [16].

2. Experiment Procedures

Analytical grade ethanol used in this study was supplied by Sinopharm Chemical Reagent Co., Ltd. Experiments were conducted at equivalence ratios of 0.6, 0.7, 0.8, 0.9, 1.0, 1.1, 1.2, 1.3 and 1.4. Before fuel injection, the chamber was vacuumed to approximately 50 kPa absolute pressure, and heated to 358 K. Fuels were then injected into the combustion chamber by micro syringes with capacities of 500 μL. Ethanol injection volumes of different equivalence ratios ϕ at the experimental conditions are calculated by Eq. (1):

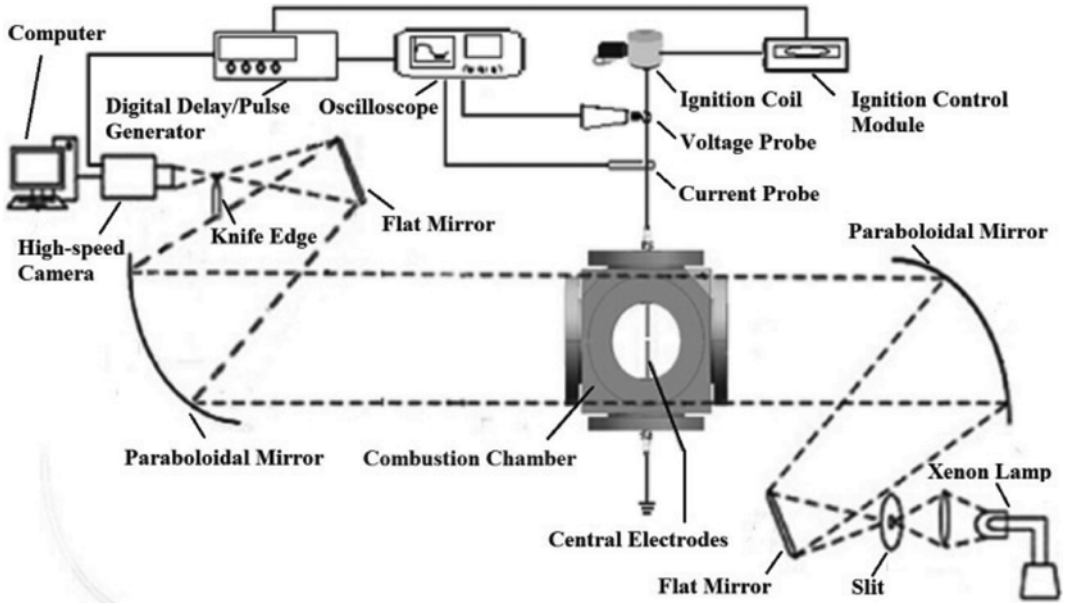

Fig. 1. Schematic diagram of experimental setup of SI.

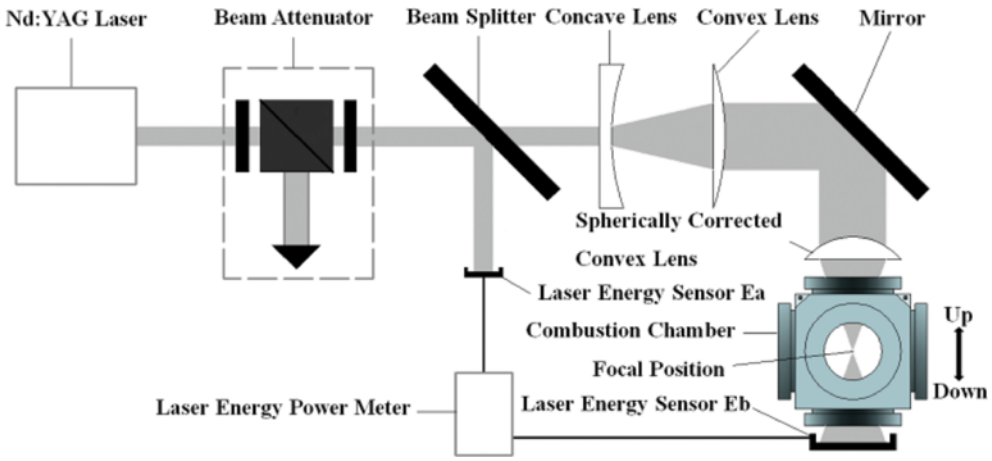

Fig. 2. Schematic diagram of experimental setup of LISI.

$$V_E = \frac{p_0 V_c M_E}{\rho_E R T_0} \frac{0.21\phi}{0.21\phi + 3} \quad (1)$$

where V_c, M_E, ρ_E, and R are volume of constant volume combustion bomb, ethanol molecular weight (46 g/mol), ethanol density (0.79 g/cm^3) at 293 K, the universal gas constant (8.314 J·mol^{-1}·K^{-1}), respectively. p_0 and T_0 represent initial pressure and initial temperature, respectively.

After fuel injection, hydrocarbon-free air was introduced. To obtain a homogeneous mixture, a standing time of at least five minutes was required before ignition. In this study, the ignition energy was fixed at 20 mJ by LISI, while the spark ignition energy was approximately 15 mJ.

Flame propagation images were recorded through a typical high-speed Schlieren photography system. The camera was operated at 6,000 fps with 512×512 pixels at a resolution of 0.237 mm/pixel. Ignition, camera and oscilloscope were triggered by a digital delay/pulse generator (SRS DG645).

All Schlieren images were processed using Photoshop software to measure the flame front area, then the flame radii were deduced.

3. Extrapolation Methodology and Data Processing

The methodology in this study to determine the laminar burning velocity is widely used in many studies [17-19]. According to the theory of outwardly propagating spherical flame, the stretched laminar flame speed S_b, referred to as flame speed hereafter, is calculated by Eq. (2):

$$S_b = \frac{dr_f}{dt} \quad (2)$$

where r_f is the flame front radius, and t is the elapsed time after ignition. The stretch rate of spherical flame κ representing the expanding rate of flame front area (A) as defined in Eq. (3):

$$\kappa = \frac{d(\ln A)}{dt} = 2\frac{S_b}{r_f} \quad (3)$$

Because the flame propagation process is affected by the stretch, and the stretch is nonlinear, we adopted the nonlinear extrapolation method to derive the unstretched flame propagation speed S_b^0. The widely used nonlinear equation, which is under an assumption of adiabatic and quasi-steady propagation, is shown in Eq. (4) [18,19]:

$$\left(\frac{S_b}{S_b^0}\right)^2 \ln\left(\frac{S_b}{S_b^0}\right)^2 = -2\frac{L_b\kappa}{S_b^0} \quad (4)$$

where L_b is the Markstein length. Generally, laminar flame speed calculated from nonlinear extrapolation is slightly smaller than that from linear extrapolation [19]. For comparing with the literature value, linear extrapolation also was adopted to calculate the flame propagation speed:

$$S_b = S_b^0 - L_b\kappa \quad (5)$$

Because pressure during the combustion of quasi-steady period can be considered as constant, the laminar burning velocity u_l can be calculated according to mass conservation by Eq. (6) [20,21]:

$$u_l = \frac{\rho_b}{\rho_u} S_b^0 \quad (6)$$

where ρ_b and ρ_u are adiabatically burned and unburned mixture densities, which can be calculated directly from the EQUIL Code of the Chemkin-Pro software.

EXPERIMENTAL RESULTS AND DISCUSSION

1. Ignition and Third Lobe Kernel

Morsy [8] and Phuoc [22] reviewed four different mechanisms by which laser light can interact with a combustible mixture to initiate an ignition event: thermal initiation, photochemical ignition, resonant breakdown, and non-resonant breakdown. The last one is generally termed as laser-induced spark ignition (LISI), which is the most frequently adopted ignition mode to initiate combustion primarily. The initiation of the breakdown process of non-resonant breakdown most likely derives from electron cascade ionization, by which initial electrons absorb photons out of the laser beam via the inverse Bremsstrahlung process [8].

Fig. 3 presents chronological Schlieren images of ethanol-air mixture at an equivalence ratio of 1.0 under an initial condition of 358 K temperature and 0.1 MPa pressure. Because of the uncertainty of LISI, the location of the ignition point is not always situated in the center of the combustion chamber. For the SI flame,

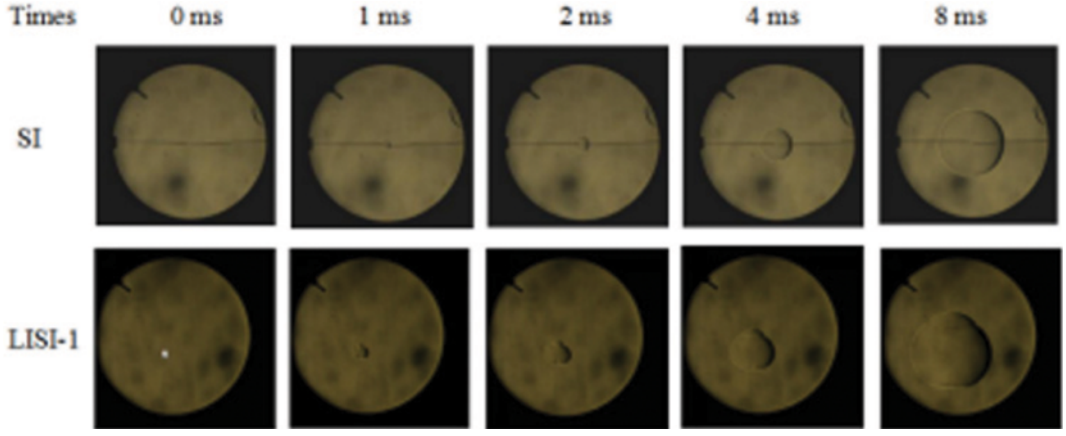

Fig. 3. Chronological Schlieren images of ethanol at an equivalence ratio of 1.0 (Initial conditions: T_0=358 K, p_0=0.1 MPa).

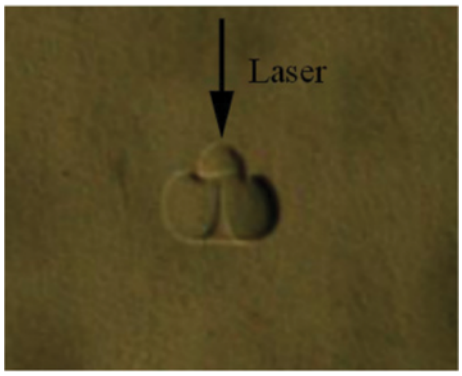

Fig. 4. Illustration of third lobe kernel.

the flame front is near-spherical, due to reduced obstructing and quenching effect by using extremely thin wires with diameters of 0.4 mm; while the flame front of LISI is not spherical due to the existence of a third lobe kernel, as shown in Fig. 4. The shape of the flame is asymmetric in the direction of the laser beam such that two distinct segments are observed during the initial flame kernel development: a torus-like shape propagating radially and a third lobe propagating back toward the laser source. The evolution of the third lobe could be due to the initial flow field created by the propagation of a radiation transport wave up the laser beam, arising from the high rate of energy transfer at the leading edge of the plasma [8,9].

2. Flame Propagation and Laminar Burning Speed

Fig. 5 presents the flame radius of ethanol ignited by SI and LISI. LISI flame propagates faster than SI flame at an equivalence ratio of 0.9 for ethanol-air mixture. At the same time, flame radius of LISI is larger than that of SI.

Fig. 6 shows the relationship between flame speeds and stretch rate with LISI and SI. The flame propagation trends are similar to the lean *n*-butane-air flame studied by Kelly and Law [19], which consists of three distinctive periods: an initial period dominated and then influenced by the ignition energy, followed by a quasi-steady period and final period influenced by chamber confinement. Because the early stage of the flame was significantly affected by the ignition energy, there were significant differences in flame size among each equivalence ratio at early flame stage. As shown in Fig. 6, flame stretch rate with LISI is greater than that with SI in the initial period. Upon ignition, the flame is initially driven by thermal conduction from the ignition kernel to the flame front. The flame speed subsequently decreases as the influence of the ignition kernel is dissipated. Then flame propagation is supported by the heat released from burned zone [19,23]. This effect will immediately diminish when the flame radius is larger than a critical radius; therefore, by properly selecting time window for analysis, the effects of ignition process are negligible in the flame propagation speed calculation. In this study, only the radius between 10 and 19 mm [19], between which the volume of burned gas is less than 1.6% chamber volume [19], was chosen for analysis.

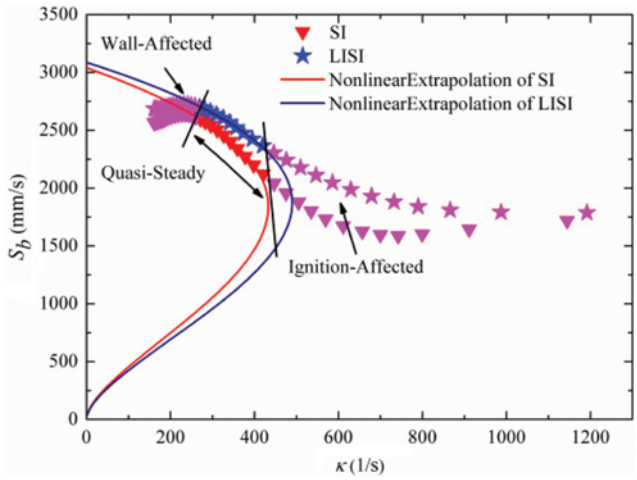

Fig. 6. Flame speed as a function of stretch for ethanol at equivalence ratio 0.9 (Initial conditions: T_0=358 K, p_0=0.1 MPa).

Fig. 7 indicates both the laminar burning velocity measurements

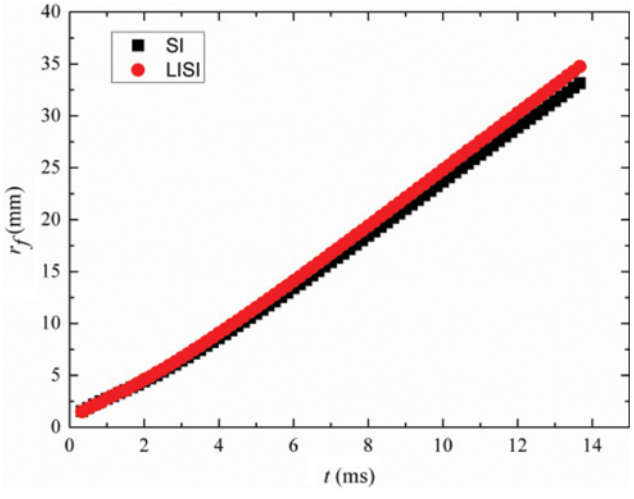

Fig. 5. Flame radius as a function of time for ethanol at equivalence ratio 0.9 (Initial conditions: T_0=358 K, p_0=0.1 MPa).

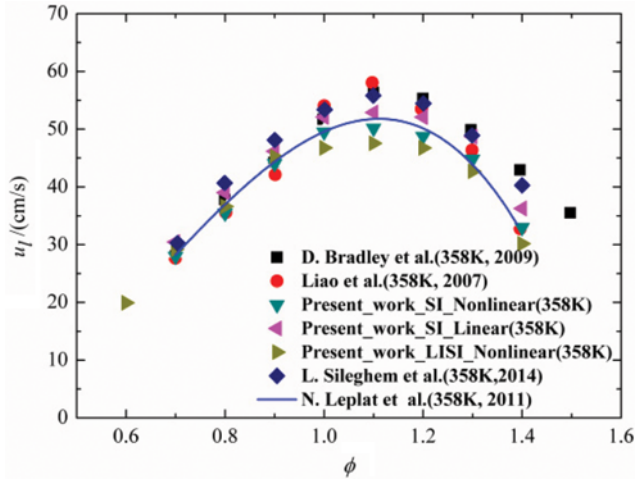

Fig. 7. Evolution of laminar burning velocity for ethanol versus the equivalence ratio and comparison of the laminar burning velocities of ethanol from the current work and other studies.

with LISI and SI. To compare with data reported in the literature, the experiment data of SI were processed by linear and nonlinear extrapolation methods. Laminar burning velocity with LISI is faster than that with SI at a lean mixture, but slower at stoichiometric and rich mixtures with nonlinear extrapolation. The peak values of the laminar burning velocity for the SI and LISI of present work with nonlinear extrapolation are 50.1 cm/s and 47.6 cm/s at the equivalence ratio of 1.1, respectively. With linear extrapolation, the maximum laminar burning velocity of ethanol-air mixture ignited by electric spark by research of Bardley et al. [25], Liao et al. [26] and Sileghem et al. [27] was 3.5 cm/s, 5 cm/s and 3 cm/s faster than that of present work at the equivalence of 1.1 under identical initial conditions, respectively. We assumed that a shock wave [9] exists along with LISI contributing to the faster and slower flame propagation at lean mixture and stoichiometric and rich mixtures, respectively. Besides, LISI can ignite the ethanol-air mixture at an equivalence ratio of 0.6 at this experiment condition; however, when ignition energy of SI is increased to 20 mJ, the ethanol-air mixture at an equivalence ratio of 0.6 cannot be ignited.

3. Radiation Effect

Chen [28] suggested that flame propagation could be affected by radiation. The reduction of the flame propagation speed was caused by the coupling between the thermal effect (change of flame temperature or unburned gas temperature) and flow effect (inward flow of burned gas) induced by radiation. Yu et al. [29] proposed an empirical formula to correct the measured laminar burning speed as follows:

$$u_l^0 = u_l + 0.82 u_l \left(\frac{u_l}{S^*}\right)^{-1.14} \left(\frac{T_0}{T^*}\right) \left(\frac{p_0}{p^*}\right)^{-0.3} \quad (7)$$

where the values of S^*, T^*, p^* are 1 cm/s, 298 K, 1 atm. From Eq. (7), the relative deviation caused by radiation can determined:

$$R_{dev} = 0.82 \left(\frac{u_l}{S^*}\right)^{-1.14} \left(\frac{T_0}{T^*}\right) \left(\frac{p_0}{p^*}\right)^{-0.3} \quad (8)$$

R_{dev} depends on the u_l, T_0 and p_0. The relative deviation increases with increasing initial temperature T_0, but decreases with increasing measured laminar burning speeds u_l and initial pressure p_0. For the present experiment, the initial condition was fixed, so the contribution to R_{dev} from initial temperature and pressure is identical. The difference of the relative deviation at each test is derived from the measured laminar burning speed of each test. The relative deviations at various equivalence ratios are shown in Fig. 8. R_{dev} first decreases then increases with increasing equivalence ratio. The maximum deviation is close to 3.25%, which means that the radiation effect in this experiment can be neglected.

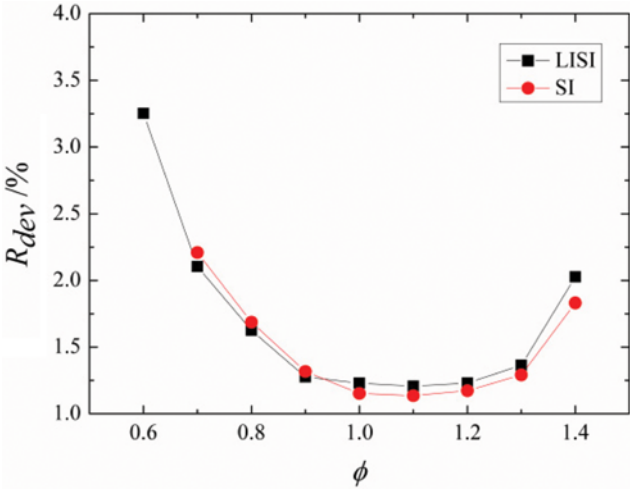

Fig. 8. Relative deviation caused by radiation for ethanol versus the equivalence ratio.

CONCLUSIONS

A comparative experimental study of ethanol-air premixed laminar combustion characteristics by laser induced spark and electric spark ignition was performed in a constant volume combustion chamber at an initial temperature of 358 K and initial pressure of 0.1 MPa. Results show that the laminar speeds of ethanol-air with LISI are faster than that with SI at lean mixture, but slower at stoichiometric and rich mixtures; the peak values of the laminar burning velocity for SI and LISI with nonlinear extrapolation are 50.1 cm/s and 47.6 cm/s at the equivalence ratio of 1.1, respectively. Besides, LISI can ignite leaner ethanol-air mixture at an equivalence ratio of 0.6. It is assumed that a shock wave exists along with the LISI, which leads to the faster and slower combustion at lean mixture and stoichiometric and rich mixtures, respectively. In the future, the shock wave along with LISI should be further studied and verified. In this study, the radiation induced relative deviation first decreased and then increased with increasing equivalence ratio, and the maximum deviation was 3.25% corresponding to equivalence ratio 0.6, which means that the radiation effect in this experiment can be neglected.

ACKNOWLEDGEMENTS

This work is supported by the National Basic Research Program (No. 2013CB228106) of China, the National Natural Science Foundation of China (No. 50976100 and 51076138), the Public Beneficial Technology Application Research Project of Science Technology Department of Zhejiang Province (No. 2016C31102 and 2016C31112), and the Fundamental Research Funds for the Central Universities (No. 2013QNA4017), China.

NOMENCLATURE AND ABBREVIATION

SI : electric spark ignition
LISI : laser induced spark ignition
ϕ : equivalence ratio
V_c : volume of the constant volume combustion bomb (L) (L)
ρ_E : density of ethanol at 293 K [g/cm^3]
M_E : molecular weight of ethanol [g/mol]
p_0 : initial pressure [Pa]
T_0 : initial temperature [K]
R : universal gas constant [J·mol^{-1}·K^{-1}]
V_E : injection volume of ethanol [μL]
r_f : flame radius [mm]
A : flame front area [mm^2]

t : elapsed time after ignition [s]
S_b : stretched flame speed [mm/s]
κ : stretch rate [s^{-1}]
S_b^0 : unstretched flame speed [cm/s]
L_b : markstein length [mm]
u_l : measured laminar burning velocity [cm/s]
ρ_b : density of burned gas [kg/m^3]
ρ_u : density of unburned gas [kg/m^3]
u_l^0 : corrected laminar burning velocity [cm/s]
R_{dev} : radiation induced relative deviation
S^* : reference speed [cm/s]
p^* : reference pressure [Pa]
T^* : reference temperature [K]

REFERENCES

1. X. Meng, H. Huang, Q. Zhang, C. Li and Q. Cui, *Korean J. Chem. Eng.*, **33**, 1239 (2016).
2. X. Qu, C. Gong, J. Liu, F. Cui and F. Liu, *Fuel*, **158**, 166 (2015).
3. W. M. Ambrós, T. D. M. Lanzanova, J. L. S. Fagundez, R. L. Sari, D. K. Pinheiro, M. E. S. Martins and N. P. G. Salau, *Fuel*, **158**, 270 (2015).
4. J. Jeong, B. Jang, Y. Kim, B. Chung and G. Choi, *Korean J. Chem. Eng.*, **26**, 1308 (2009).
5. R. Da Silva, R. Cataluña, E. W. D. Menezes, D. Samios and C. M. S. Piatnicki, *Fuel*, **84**, 951 (2005).
6. P. Dirrenberger, P. A. Glaude, R. Bounaceur, H. Le Gall, A. P. Da Cruz, A. A. Konnov and F. Battin-Leclerc, *Fuel*, **115**, 162 (2014).
7. R. C. Costa and J. R. Sodré, *Fuel*, **89**, 287 (2010).
8. M. H. Morsy, *Renew. Sust. Energy Rev.*, **16**, 4849 (2012).
9. D. Bradley, C. G. W. Sheppard, I. M. Suardjaja and R. Woolley, *Combust. Flame*, **138**, 55 (2004).
10. D. K. Srivastava, M. Weinrotter, K. Iskra, A. K. Agarwal and E. Wintner, *Int. J. Hydrogen Energy*, **34**, 2475 (2009).
11. V. Tihay, P. Gillard and D. Blanc, *J. Hazard. Mater.*, **209-210**, 372 (2012).
12. D. B. Ker and D. Brüggemann, *Int. J. Hydrogen Energy*, **36**, 14759 (2011).
13. M. Weinrotter, H. Kopecek, E. Wintner, M. Lackner and F. Winter, *Int. J. Hydrogen Energy*, **30**, 319 (2005).
14. J. X. Ma, D. R. Alexander and D. E. Poulain, *Combust. Flame*, **112**, 492 (1998).
15. K. M. Rahman, N. Kawahara, K. Tsuboi and E. Tomita, *Fuel*, **165**, 331 (2016).
16. C. Xu, D. Fang, Q. Luo, J. Ma and Y. Xie, *Optics Laser Technology*, **64**, 343 (2014).
17. T. Tahtouh, F. Halter and C. Mouna M-Rousselle, *Combust. Flame*, **156**, 1735 (2009).
18. E. Varea, V. Modica, A. Vandel and B. Renou, *Combust. Flame*, **159**, 577 (2012).
19. A. P. Kelley and C. K. Law, *Combust. Flame*, **156**, 1844 (2009).
20. F. N. Egolfopoulos, N. Hansen, Y. Ju, K. Kohse-H Inghaus, C. K. Law and F. Qi, *Prog. Energy Combust. Sci.*, **43**, 36 (2014).
21. G. Broustail, F. Halter, P. Seers, G. Moréac and C. Mouna M-Rousselle, *Fuel*, **106**, 310 (2013).
22. T. X. Phuoc, *Opt. Laser. Eng.*, **44**, 351 (2006).
23. Z. Chen, *Combust. Flame*, **162**, 2442 (2015).
24. G. Dayma, F. Halter, F. Foucher, C. Mounaim-Rousselle and P. Dagaut, *Energy Fuel*, **26**, 6669 (2012).
25. D. Bradley, M. Lawes and M. S. Mansour, *Combust. Flame*, **156**, 1462 (2009).
26. S. Y. Liao, D. M. Jiang, Z. H. Huang, K. Zeng and Q. Cheng, *Appl. Therm. Eng.*, **27**, 374 (2007).
27. L. Sileghem, V. A. Alekseev, J. Vancoillie, E. J. K. Nilsson, S. Verhelst and A. A. Konnov, *Fuel*, **115**, 32 (2014).
28. Z. Chen, *Combust. Flame*, **157**, 2267 (2010).
29. H. Yu, W. Han, J. Santner, X. Gou, C. H. Sohn, Y. Ju and Z. Chen, *Combust. Flame*, **161**, 2815 (2014).